Organic & Biomolecular Chemistry

This article is part of the

OBC 10th anniversary

themed issue

All articles in this issue will be gathered together online at

www.rsc.org/OBC10

Organic & Biomolecular Chemistry

Cite this: *Org. Biomol. Chem.*, 2012, **10**, 6217

www.rsc.org/obc

PAPER

Structure, stereochemistry and synthesis of enantiopure cyclohexenone *cis*-diol bacterial metabolites derived from phenols†‡

Derek R. Boyd,*[a] Narain D. Sharma,[a] John F. Malone,[a] Peter B. A. McIntyre,[a] Paul J. Stevenson,[a] Christopher C. R. Allen,[b] Marcin Kwit[c] and Jacek Gawronski*[c]

Received 11th January 2012, Accepted 22nd February 2012
DOI: 10.1039/c2ob25079a

Biotransformation of 3-substituted and 2,5-disubstituted phenols, using whole cells of *P. putida* UV4, yielded cyclohexenone *cis*-diols as single enantiomers; their structures and absolute configurations have been determined by NMR and ECD spectroscopy, X-ray crystallography, and stereochemical correlation involving a four step chemoenzymatic synthesis from the corresponding *cis*-dihydrodiol metabolites. An active site model has been proposed, to account for the formation of enantiopure cyclohexenone *cis*-diols with opposite absolute configurations.

1. Introduction

Phenols are major aromatic metabolites formed *via* hydroxylase-catalysed monohydroxylation, monooxygenase-catalysed epoxidation (followed by spontaneous isomerisation), and dioxygenase-catalysed *cis*-dihydroxylation of arenes followed by spontaneous dehydration.[1a] The metabolic fate of phenols is thus an important topic, particularly in the environment. The bacterial monohydroxylation of phenols **1** to yield catechols **2**,[1a–k] and hydroquinones **3**,[1j,k] has been widely recognized as a major mineralization pathway in the environment (Scheme 1). Recent studies in these laboratories have focused on new families of chiral metabolites from phenol substrates **1** using mutant and recombinant bacterial strains.[2a–c] In this context, 3-substituted phenols **1** (R′ = H) were found to adopt *cis*-dihydroxylation pathways involving toluene dioxygenase (TDO)-catalysed oxidation to yield the corresponding, relatively stable, cyclohexenone *cis*-diols $\mathbf{4}_S$ as single enantiomers.[2a–c] The latter type of *cis*-diols, often formed in modest yields, has received little attention compared with the corresponding less stable benzene *cis*-dihydrodiols **6**[3a–n] from non-phenolic substrates.

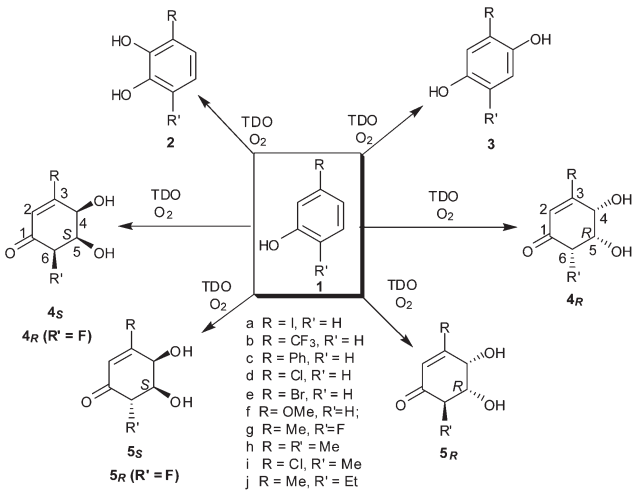

Scheme 1 Biotransformation products obtained from substituted phenols using *P. putida* UV4.

The cyclohexenone *cis*-diol bioproducts **4** (R′ = H), derived from the TDO-catalysed biotransformation of 3-substituted phenols **1** (R′ = H) in whole cells of *P. putida* UV4, were found to be enantiopure, and of identical (5*S*) absolute configuration.[2a–c] Surprisingly, the 2,5-disubstituted phenol, *p*-xylenol **1** (R = R′ = Me), also gave a cyclohexenone *cis*-diol **4** (R = R′ = Me) as a single cyclohexenone *cis*-diol diastereoisomer (>98% ee) but had the opposite (5*R*) absolute configuration compared with cyclohexenone *cis*-diol metabolites derived from 3-substituted phenols.[2a] The objectives of the current study were to: (i) extend the range of substituted phenol substrates **1**, found to undergo dioxygenase-catalysed *cis*-dihydroxylation using whole cell cultures of *P. putida* UV4, and provide evidence of the general applicability of this new metabolic pathway to other

[a]*School of Chemistry and Chemical Engineering, Queen's University, Belfast, BT9 5AG, UK. E-mail: dr.boyd@qub.ac.uk; Fax: +44 (0) 28 9097 4687; Tel: +44 (0) 28 9097 4421*
[b]*School of Biological Sciences, Queen's University, Belfast BT9 7BL, UK*
[c]*Department of Chemistry, A. Mickiewicz University, Grunwaldzka 6, 60–780 Poznan, Poland. E-mail: gawronsk@amu.edu.pl; Fax: (+48)-61-8658-008*

†This article is part of the *Organic & Biomolecular Chemistry* 10th Anniversary issue.

‡Electronic supplementary information (ESI) available. CCDC 852568, 852569 and 852570. For ESI and crystallographic data in CIF or other electronic format see DOI: 10.1039/c2ob25079a

types of chiral cyclohexenone *cis*-diols (*e.g.* **4** and **5**), (ii) carry out full structural and stereochemical characterizations of new cyclohexenone *cis*-diol diastereoisomers (**4** and **5**) and enantiomers having opposite absolute configurations ($\mathbf{4}_R/\mathbf{4}_S$ and $\mathbf{5}_R/\mathbf{5}_S$) based on ECD spectroscopy, X-ray crystallography and stereochemical correlation methods, (iii) develop a chemoenzymatic synthetic route to cyclohexenone *cis*-diols $\mathbf{4}_S$ (R′ = H) from enantiopure substituted benzene *cis*-dihydrodiol precursors **6** of established absolute configuration which were readily available in multigram quantities (iv) rationalize the formation of enantiopure cyclohexenone *cis*-diol metabolites $\mathbf{4}_S$ and $\mathbf{4}_R$ of opposite absolute configurations, following TDO-catalysed *cis*-dihydroxylation of the corresponding aromatic substrates **1** and provide a simple predictive active site model.

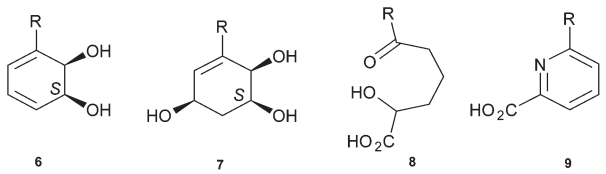

2. Results and discussion

2.1 TDO-catalysed biotransformation of phenols 1d–1g, 1i and 1j to yield the corresponding cyclohexenone *cis*-diols 4d–4g, 4i, 4j, 5g and 5i

The phenol substrates **1** and catechol bioproducts **2** for this study were available either commercially or from earlier studies.[4,5] 3-Iodophenol **1a**, 3-trifluoromethyl phenol **1b**, 3-phenylphenol **1c** and 2,5-dimethylphenol **1h** had been used earlier as substrates for *P. putida* UV4 and the corresponding cyclohexenone *cis*-diols $\mathbf{4a}_S$–$\mathbf{4c}_S$ and $\mathbf{4h}_R$ were isolated and characterized.[2a–c] These *cis*-diols have been included in Scheme 1, to allow comparison of their calculated and experimentally recorded ECD spectra (Fig. 2) with those of the new *cis*-diol bioproducts **4d**–**4g**, **4i**, **4j**, **5g** and **5i** from the corresponding phenol substrates **1d**–**1g**, **1i** and **1j**.

The earlier study[2a] had shown that biotransformation of 3-iodophenol **1a** with *P. putida* UV4 yielded cyclohexenone *cis*-diol $\mathbf{4a}_S$ as a major metabolite and only traces of catechol **2a**. The yields of cyclohexenone *cis*-diol metabolite $\mathbf{4a}_S$, formed from phenol **1a**, were found to vary greatly among repeated biotransformations. This may have been the result of several competing reactions occurring simultaneously, *e.g.* (a) reduction of the keto group in compound $\mathbf{4a}_S$ to form *cis*,*cis*-triol **7a**, (b) formation of dehalogenation products and their derivatives, (c) catechol **2a** formation which could have inhibited TDO activity.[2a,c] The reduction of the keto group was particularly favoured during the biotransformation of 3-trifluoromethylphenol **1b**, using *P. putida* UV4, where cyclohexenone *cis*-diol $\mathbf{4b}_S$ was formed and then rapidly reduced to give *cis*,*cis*-triol **7b** as the major bioproduct.[2c]

While the phenol ring of substrate **1c** was also *cis*-dihydroxylated, using *P. putida* UV4 to yield the corresponding cyclohexenone *cis*-diol $\mathbf{4c}_S$, only traces of catechol bioproduct **2c** were detected. However, it was found that a ring opening reaction of catechol **2c** had occurred to yield the acyclic ketocarboxylic acid **8c** and picolinic acid **9c** as minor metabolites.[2c] The biotransformation of phenol **1c** also gave a *cis*-dihydrodiol product **6** (R = 3–HO·C_6H_4) from oxidation of the unsubstituted phenyl ring, thus reducing the isolated yield of cyclohexenone *cis*-diol $\mathbf{4c}_S$. The formation of metabolite $\mathbf{4c}_S$ was noteworthy, since it confirmed that a member of the cyclohexenone *cis*-diol family could be formed using different types of arene dioxygenases, *e.g.* TDO, naphthalene dioxygenase and biphenyl dioxygenase.[2c]

Following on from the use of 3-iodophenol **1a** as substrate for TDO,[2a–c] during this study several other halogenated phenols were examined as substrates with *P. putida* UV4. Surprisingly, addition of 3-fluorophenol **1** (R = F, R′ = H) as substrate produced no evidence of cyclohexenone *cis*-diol **4** (R = F, R′ = H) being formed; the corresponding catechol **2** (R = F, R′ = H) was the only identified metabolite. When 3-chlorophenol **1d** and 3-bromophenol **1e** were used as substrates, the corresponding catechols **2d** and **2e** again proved to be the major bioproducts with cyclohexenone *cis*-diols **4d** and **4e** as minor products in relatively low isolated yields (≤5%). This prompted us to develop a chemoenzymatic route to these minor metabolites from the readily available *cis*-dihydrodiols **6d** and **6e** (see Section 2.3).

It was difficult to obtain accurate estimates of the relative yields of halogenated cyclohexenone *cis*-diols **4** and catechols **2** since: (i) further metabolism often occurred to different degrees among repeat biotransformations and (ii) LC-TOFMS analysis was unsuitable for the detection of catechols, and NMR spectroscopic analysis of the crude mixture of products, in some cases, proved to be less reliable due to the presence of both unreacted substrates and aromatic products. Despite these limitations, a qualitative estimate based on NMR spectroscopic analysis can be made of the relative proportions of cyclohexenone *cis*-diols **4a**, **4d**, **4e** and the corresponding catechols **2a**, **2d**, **2e** obtained by TDO-catalysed oxidation. Thus, it was observed that higher yields of cyclohexenone *cis*-diols were generally obtained when using phenol substrates with larger substituents, including halogen atoms *i.e.* **4a** > **4e** > **4d** > **4** (R = F, R′ = H). As already mentioned in the context of metabolite **4a**,[2a,c] and in view of conversion of substrate generally being complete, the variable yields of cyclohexenone *cis*-diols obtained herein are mainly assumed to result from further metabolism or alternative metabolic pathways to give water-soluble products.

Methoxyphenols are commonly found in ecosystems as natural and combustion products derived from plants, as well as from anthropogenic sources. As the initial step of a wider programme to investigate the dioxygenase-catalysed biotransformation of methoxyphenols, including those found in the environment, 3-methoxyphenol **1f** was examined as a substrate for *P. putida* UV4. It was gratifying to find that the isolated yields of cyclohexenone *cis*-diol **4f**, using substrate **1f**, were consistently higher (>50%) than those obtained with halogenated phenols **1d** and **1e** and most other 3-substituted phenols. Although little evidence was found for the formation of catechol **2f**, a minor unidentified bioproduct was also detected and separated during purification of *cis*-diol **4f**. The structures of cyclohexenone *cis*-diols **4d**, **4e** and **4f** were established by a combination of spectroscopic and chiroptical methods that had

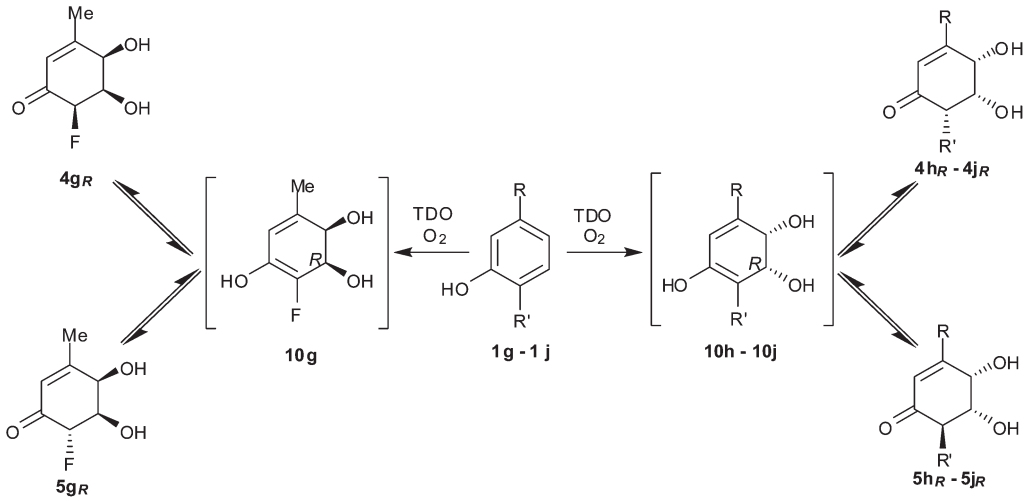

Scheme 2 TDO-catalysed formation of *cis*,*cis*-**4g$_R$**–**4j$_R$** and *cis*,*trans*-cyclohexenone diols **5g$_R$**–**5j$_R$** from the initial *cis*-dihydrodiol intermediates **10g$_R$**–**10j$_R$** and phenol substrates **1g**–**1j**.

been used earlier for the other members of this family of metabolites.[2a–c]

Due to the remarkable stability of *cis*-diol **4f**, compared to the methoxy substituted *cis*-dihydrodiol metabolite **6f** derived from methoxybenzene,[5] and the reproducible yields recorded during shake flask biotransformations, large-scale (>100 litre) biotransformation studies are in progress to optimize the yield and obtain multigram quantities for examination of its potential as a multifunctional chiral precursor in chemoenzymatic synthesis.

The earlier communication on this study[2a] showed that TDO-catalysed *cis*-dihydroxylation of 2,5-dimethylphenol **1h** (a metabolite of *p*-xylene) by *P. putida* UV4 yielded metabolite **4h$_R$**, as the first disubstituted member of the cyclohexenone *cis*-diol family. With most of the other previously reported cyclohexenone *cis*-diol metabolites having been derived from monosubstituted phenols,[2a–c] cyclohexenone *cis*-diol **4h$_R$** was the first member of this family to possess three endocyclic chiral centres. X-ray crystallography and NMR spectroscopic analysis of a monocamphanate derivative showed that the two hydroxyl groups (at C4 and C5) and the methyl group (at C6) had a *cis*,*cis* relationship in metabolite **4h$_R$**.[2a]

Three more 2,5-disubstitututed phenols **1g**, **1i** and **1j** have now been found to be acceptable substrates for *P. putida* UV4. The corresponding cyclohexenone *cis*-diols **4g$_R$**, **4i$_R$**, **4j$_R$** were identified as major metabolites, initially on the basis of NMR spectroscopy (Scheme 2). The *cis*,*cis* metabolites **4h$_R$** and **4j$_R$**, appeared to be the only identified cyclohexenone *cis*-diols present in the crude mixtures. However, a careful analysis of the NMR spectra of the crude mixture, recorded immediately after biotransformation of phenols **1h** and **1j**, also showed traces of the minor diastereoisomers **5h$_R$** and **5j$_R$**, which disappeared during isolation of the major metabolites **4h$_R$** and **4j$_R$**, presumably *via* epimerization. This premise was supported when the two *cis*,*trans* diastereoisomers **5g$_R$** and **5i$_R$** were found as significant minor metabolites (30% and 10% relative yields respectively) in the crude culture media and were readily separable from the major cyclohexenone *cis*-diols **4g$_R$** and **4i$_R$** by PLC.

The relative configuration of cyclohexenone *cis*-diol **4h$_R$** had been established earlier by X-ray crystal structure analysis.[2a] It indicated a preference for the half-chair conformation and a *cis*, *cis* relationship between substituents *i.e.* (pseudo)equatorial C4–OH and C6–Me and a (pseudo)axial C5–OH. It is probable that this is also the preferred conformation in a solution of the *cis*-diol moiety in metabolites **4a**–**4j**, based on NMR spectroscopy analysis. The structures of all the cyclohexenone *cis*-diols shown in Scheme 1 (**4a$_S$**–**4f$_S$**, **4g$_R$**–**4j$_R$**, **5g$_R$** and **5i$_R$**) were assigned using a combination of NMR spectroscopy and mass spectrometry. The vicinal coupling constants $J_{4,5}$ were consistently located within the range found earlier for the *cis*-diol configuration among other members of this family of metabolites (2.5–3.6 Hz).[2a–c] The ^{1}H coupling constant values at C6 and C5, *i.e.* $J_{5,6}$ = 2.6, in *cis*-diol **4g** and 2.3 in *cis*-diol **4i**, were consistent with a *cis* relationship. The larger *trans* C5–C6 coupling constants found in *cis*-diols **5g** and **5i** ($J_{5,6}$ = 10.3 and 8.4 Hz respectively) were consistent with C5 and C6 substituents adopting (pseudo)equatorial conformations and C4 a (pseudo)axial conformation.

The major *cis*,*cis*-diastereoisomers **4g**–**4j** showed little evidence of epimerization in $CDCl_3$ or D_2O solution at ambient temperature over an extended period (>10 days). This contrasted with the behaviour of the minor halogenated *cis*,*trans* metabolites **5g** and **5i** which in $CDCl_3$ solution, were observed to epimerize *via* an inversion of configuration at the C6 chiral centre, over a period of several days, to yield the corresponding *cis*,*cis* diastereoisomers **4g** and **4i** (Scheme 2). This observation suggested that both the *cis*,*cis* isomers **4g** and **4i** and the corresponding *cis*,*trans* diastereoisomers **5g** and **5i** were formed simultaneously under kinetic control in the aqueous culture medium. Equilibration could then occur *via* undetected enol intermediates **10g** and **10i** with the less stable *cis*,*trans* isomers epimerizing to give the thermodynamically preferred *cis*,*cis* isomers **4g** and **4i** in $CDCl_3$ solution.

The cyclohexenone *cis*-diols chlorosphaeropsidone **5k** and *epi*-chlorosphaeropsidone **4k** have been isolated as natural products from cultures of *Sphaeropsis sapinea f. sp. Cupressi*, a fungus responsible for canker among cypress trees (Scheme 3).[6a] Compounds **4k** and **5k**, although possibly derived from epoxide precursors,[6a,b] were found to have very similar structures to

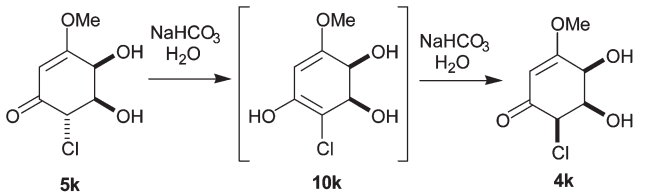

Scheme 3 Base-catalysed epimerization of chlorosphaeropsidone **5k** to epi-chlorosphaeropsidone **4k**.

cyclohexenone *cis*-diol metabolites $\mathbf{4g}_{R}$–$\mathbf{4j}_{R}$, $\mathbf{5g}_{R}$ and $\mathbf{5i}_{R}$ derived from phenol precursors (Scheme 3). The *cis*,*trans* metabolite **5k** was found to epimerize to *cis*,*cis* isomer **4k** *via* the undetected enol tautomer **10k**.[6] The relative configuration of compound **5k** in the solid state was provided by X-ray crystallography with (pseudo)equatorial C5–OH and C6–Cl substituents and a (pseudo)axial C4–OH substituent. Based on NMR coupling constants, this also appeared to be the preferred conformation in $CDCl_3$ solution.[6a]

The preference for *cis*,*cis* isomers **4g–4k** at equilibrium may result from reduced repulsive interactions of the 4,6-(pseudo) diaxial C4–H and C6–H atoms compared with the stronger 4,6-(pseudo)diaxial C4–OH and C6–H interactions associated with the preferred conformation of *cis*,*trans* isomers **5g–5k**.

Earlier attempts to detect the initial *cis*-dihydrodiol (enol) metabolite **10a** from TDO-catalysed *cis*-dihydroxylation of phenol **1a**, either by formation of a diene cycloadduct (using 4-phenyl-1,2,4-triazoline-3,5-dione as dienophile), or by trapping as an enol ether using diazomethane as methylating agent, were unsuccessful.[2a] The preferential formation of *cis*,*cis* diastereoisomers **4g–4k** and epimerization of the corresponding *cis*,*trans* isomers **5g–5k** provide strong evidence that the undetected enols **10g–10k** were indeed the initial phenol metabolites and were responsible for *cis*/*trans* isomerization.

In all cases the new cyclohexenone *cis*-diol metabolites **4d–4g**, **4i**, **4j**, **5g** and **5j** were found to be enantiopure (>98% ee) by ^{1}H NMR analysis of the corresponding chiral boronate derivatives which formed readily when mixed with (*R*)- and (*S*)-2−(1-methoxyethyl)benzeneboronic acid. This method has been used successfully for other cyclohexenone *cis*-diols **4**[2a–c] and also for a wide range of benzene *cis*-dihydrodiols **6**.[7a–c]

2.2 Absolute configuration determination of cyclohexenone *cis*-diols $\mathbf{4a}_{S}$–$\mathbf{4f}_{S}$, $\mathbf{4g}_{R}$–$\mathbf{4j}_{R}$, $\mathbf{5g}_{R}$ and $\mathbf{5i}_{R}$ by X-ray crystallography and chiroptical methods

(i) X-ray crystallography. Only the relative configuration of cyclohexenone *cis*-diol $\mathbf{4g}_{R}$ was assigned by X-ray crystallography (Fig. 1). The absolute configuration was obtained from monocamphanate derivative $\mathbf{4g}_{R\text{-cam}}$ following reaction with (−)-(*S*)-camphanic chloride. The cyclohexenone *cis*-diols $\mathbf{4g}_{R}$ and $\mathbf{4i}_{R}$, were assigned 4*R*,5*R*,6*R* and 4*R*,5*R*,6*S* configurations respectively by X-ray crystallography (Fig. 1). While compounds $\mathbf{4g}_{R}$ and $\mathbf{4i}_{R}$ were shown to have opposite absolute configurations at both C4 and C5, application of the Sequence Rule resulted in an *R* configuration at C5 in each case due to a priority change. Compounds $\mathbf{4g}_{R}$, $\mathbf{4i}_{R}$ and $\mathbf{4g}_{R\text{-cam}}$ do not show any intramolecular hydrogen bonding in the solid state, where intermolecular

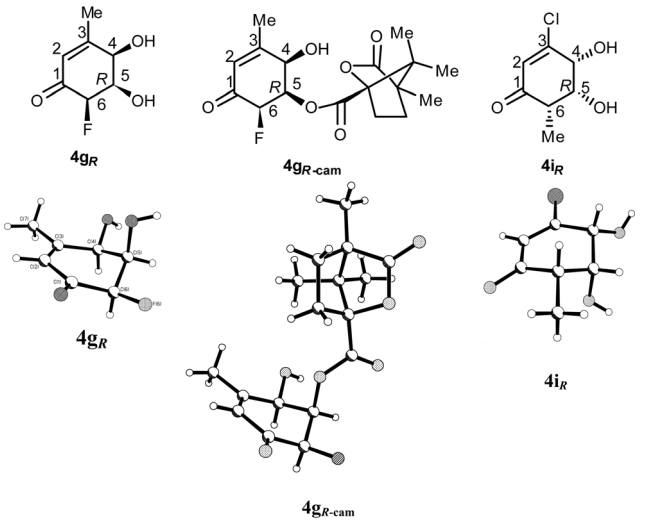

Fig. 1 Cyclohexenone *cis*-diol relative ($\mathbf{4g}_{R}$) and absolute ($\mathbf{4g}_{R\text{-cam}}$, and $\mathbf{4i}_{R}$) configuration assignments by X-ray crystallography.

interactions in crystal growth are likely to dominate. Thus, all hydroxyl, and some keto, groups are involved in extensive intermolecular hydrogen bonds.

(ii) Electronic circular dichroism spectroscopy (ECD) and specific optical rotation (OR) measurements. The absolute configurations of the new metabolites **4a–4g**, **4i**, **5g** and **5i** were independently assigned using ECD spectroscopy. While the ECD spectra and absolute configurations of cyclohexenone *cis*-diols $\mathbf{4h}_{R}$ and $\mathbf{4j}_{R}$ have been reported,[2b] full characterization data for compound $\mathbf{4j}_{R}$ was not available earlier, and has now been included in the experimental section. It has been demonstrated that electronic circular dichroism spectra and optical rotation values, obtained by comparison of experimental measurements and by calculations provide a reliable and generally applicable method for the determination of absolute configurations of synthetic and natural chiral compounds including *cis*-dihydrodiols.[7a–c]

Compounds having an enone chromophore occupy a special position, due to their occurrence in many important polycyclic molecules, *e.g.* steroidal hormones. For correlation of the observed chiroptical phenomena with the structure, two fundamental contributions have to be taken into account: first – the intrinsic helicity of the enone chromophore, and second – the extrachromophoric perturbation (substitution pattern). As both the helicity of the chromophore and the substituents contribute to the Cotton effect, it is important to determine the dominant contribution. During the last decades various chirality rules have been proposed to correlate the chiroptical properties of α,β-unsaturated ketones with their stereochemistry.[8a–v] However, until now there has been no general empirical rule which unambiguously accounts for all chiroptical phenomena observed for enones, thus theoretical support seems to be mandatory.

We have successfully applied this experimental/theoretical approach to several alkyl-substituted cyclohexenone-*cis*-diol metabolites $\mathbf{4}_{R}$ (R = Me, Et, *i*-Pr, t-Bu, R′ = H), $\mathbf{4h}_{R}$ and $\mathbf{4j}_{R}$.[2b] The latter study focused mostly on the factors that control the structure and chiroptical properties of substituted 2-

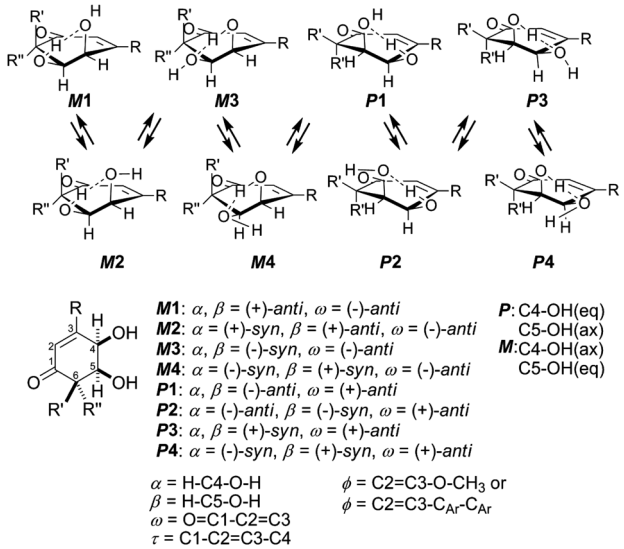

Scheme 4 Diastereoisomeric *P* and *M* conformers of *cis*-ketodiols **4a**–**4g**, ***ent*-4j**, **5g** and ***ent*-5i** and the definition of torsion angles α, β, ϕ and ω, τ (see ESI‡ for details).

cyclohexenones and resulted in redefinition of the role of substituents and 2-cyclohexenone conformation in electronic circular dichroism spectra. It has been found that non-planarity of the C=C double bond and the presence of an equatorial hydroxy group in the allylic position affected the ECD spectra most significantly. Another result of our study was the determination of the nature of the first three bands in the ECD spectra of 2-cyclohexenones. In the case of hydroxy-substituted 2-cyclohexenones, the long-wavelength electronic transition originates from the $n_{C=O}$–$\pi_{C=O}$* and the second from the $\pi_{C=C}$–$\pi_{C=O}$* electronic transition whereas the third transition is due to the presence of the substituent and is of the n_{OH}–$\pi_{C=O}$* type.[2b] It seemed reasonable that this approach could also be applied to the assignment of absolute configurations of the new members of the cyclohexenone *cis*-diol family **4a**$_S$–**4f**$_S$, **4g**$_R$–**4j**$_R$, **5g**$_R$ and **5i**$_R$ with either heteroatom or π-conjugated substituents in C3 or C6 positions.

In order to determine the chiroptical properties of enones **4a**–**4g**, ***ent*-4i**, **5g** and ***ent*-5i** with a sufficient level of confidence, their structures and conformational equilibria were calculated at PCM/B2PLYP/Aug-cc-pVTZ//PCM/B3LYP/6311++G(2d,2p) level (see ESI,‡ for details). Calculations included both the ring conformers and the substituent rotamers. As shown in Scheme 4 for the assumed 5*S* (or 5*R* in the case of compounds **4g** and **5g**) absolute configuration, each ring conformation could be described as either *M* (torsion angles C3–C4–C5–C6 negative, C4–C5–C6–C1 positive, (pseudo)axial C4–OH, (pseudo)equatorial C5–OH or *P* (torsion angle C3–C4–C5–C6 positive, C4–C5–C6–C1 negative, (pseudo)equatorial C4–OH, (pseudo)axial C5–OH), according to the previous proposal.[2b] Calculated structures of individual low-energy conformers of these enones (see ESI‡) are described as sofa S(5) of either *M* or *P* helicity (Scheme 4), with various degrees of distortion from the ideal form, in the direction of a distorted half-chair (HC) conformer.

As in the case of non-phenolic arene-*cis*-dihydrodiol metabolites **6**,[7a] the number of available conformers is not limited to the *M* and *P* diastereoisomeric structures. Intramolecular hydrogen bond patterns of the hydroxy groups further increase the number of distinct stereoisomeric structures (Scheme 4). Thus, either C4–OH or C5–OH can be a hydrogen bond donor and the orientation of the O–H bond against the vicinal C–H bond can be either *syn* or *anti* (as shown by the corresponding torsion angles α and β). Up to eight conformers (*M*1–*M*4, *P*1–*P*4) are available but this number can still be larger if one includes the rotamers due to non-spherical substituents in the ring (torsion angle ϕ), *e.g.* phenyl (**4c**) or methoxy (**4f**). Calculated torsion angles α and β fall into the range ±(155°–180°) for *anti* rotamers and the range is wider for the *syn* rotamers ±(15°–87°). For the majority of cases the intramolecular hydrogen bond O–H···O is weak (calculated length 2.50 ± 0.15 Å). However, in several conformers of enones this bond is substantially shorter (2.12–2.34 Å). In these conformers the equatorial hydroxy group is a donor to the axial oxygen atom. Another exception from the general scheme was found in the cases of **4a**, ***ent*-4i**, ***ent*-5i** and *P*3–*P*4 conformers of **4c**, where again the hydrogen bond is shorter (the shortest value 2.12 Å was calculated for ***ent*-5i**) and thus it is stronger.

The distribution of conformers for each ketodiol has been calculated for a polar medium *i.e.* acetonitrile or methanol, since all the measurements of chiroptical properties were done in polar solvents.

In contrast with the C3-alkyl-substituted 2-cyclohexenone-*cis*-diols having 4*R*,5*S* configuration shown in Scheme 4 (R′ and R″ = H), where calculations indicate a strong preference of ring *P* helicity, 3-heteroatom-substituted analogs do not follow any general trend. It is apparent that the presence of a heteroatom at the C3 position affects the conformational equilibrium. Conformers of *P*-type were found as the energetic minima in the case of **4a**, **4c**–**4g**, ***ent*-4i** and ***ent*-5i** whereas for the other cyclohexenone *cis*-diols, conformers of *M*-type dominate. The presence of a polar group next to the allylic hydroxy group suggests that the interaction between both groups affects the conformation. Attractive dipole–dipole interactions between the (pseudo)axial hydroxy group and a polar substituent were found in the cases of **4f**(*M*2), ***ent*-5i**(*M*2) and **4g**(*P*2), whereas in the case of **4b**(*M*2) the structure of this conformer appears to be stabilized by the formation of a diad of the hydrogen bonds $O_{eq}H\cdots O_{ax}H\cdots FCF_2$, as in the case of other arene metabolites.[7a] The formation of hydrogen bond diads $O_{ax}H\cdots O_{eq}H\cdots F$ shifts the conformational equilibrium to *M*3 in the case of **5g**

ECD spectra of substituted 2-cyclohexenones **4a**–**4j**, **5g** and **5i**, of assumed 5*S* (or 5*R* in the case of **4g** and **5g**) absolute configuration, were calculated at the PCM/TDDFT/B2LYP/Aug-cc-pVTZ level of theory for each conformer of the relative energy within a 0–2 kcal mol^{-1} window (see ESI‡). After Boltzmann averaging and Gaussian curve fitting[9a,b] the calculated ECD spectra were compared with the experimental ones, as shown in Fig. 2. The calculated ECD curves were wavelength-corrected to match the experimental and calculated UV maxima of the strong π–π* absorption at *ca.* 220 nm (scaling factors ranged from 1.11 for **4a** to 1.15 for **4c**). This procedure still left several of the calculated ECD curves 10 nm blue-shifted, again in agreement with the previous findings. In general, the calculated ECD spectra of the majority of cyclohexenone *cis*-diols were quite similar to the experimental ones, allowing an

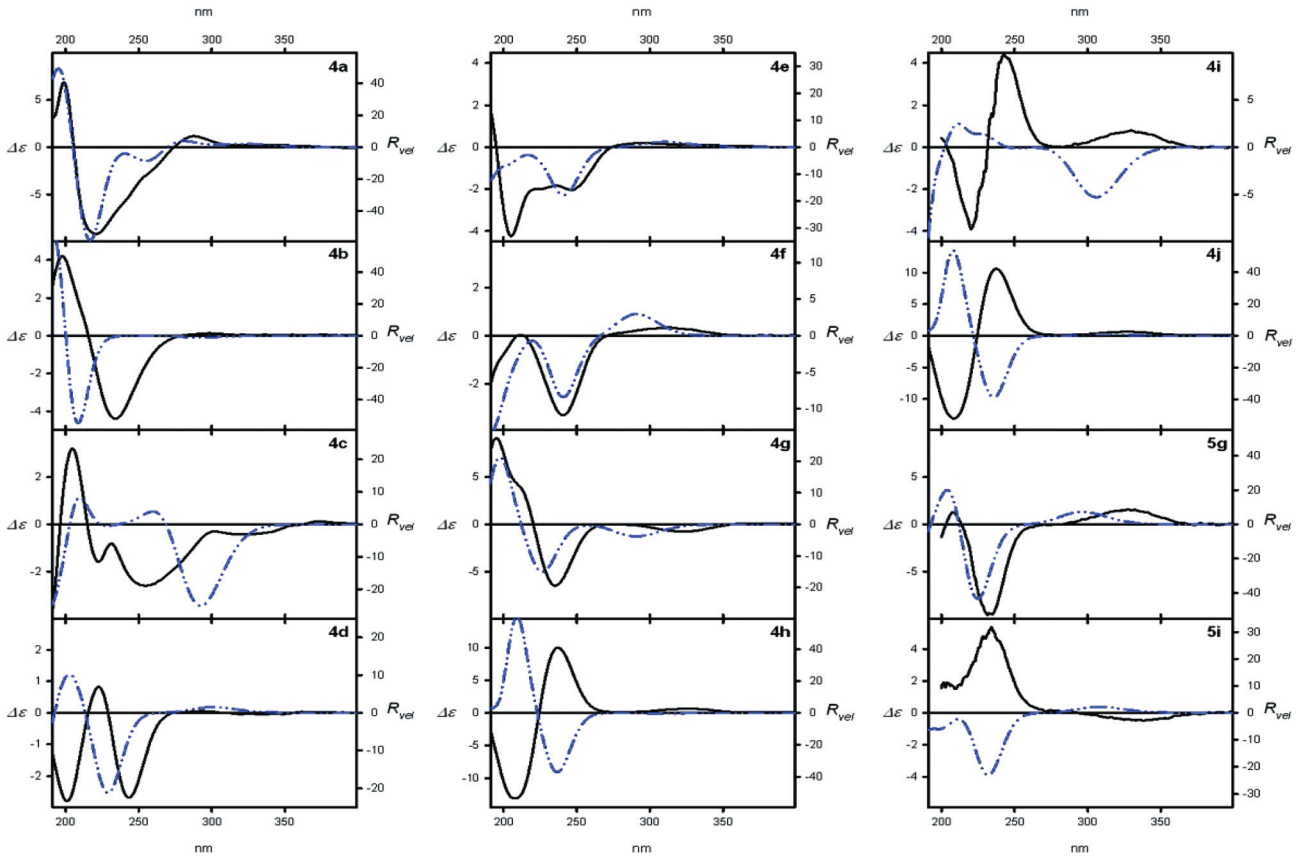

Fig. 2 ECD spectra of *cis*-ketodiols **4a–4j**, **5g** and **5i**, experimental (in acetonitrile solutions, solid lines) and $\Delta E_{B2PLYP(D)}$ Boltzmann averaged calculated at PCM/B2LYP/Aug-cc-pVTZ level (dash-dot-dot lines). Rotatory strengths *R* were calculated in dipole-velocity representation. All calculated spectra were wavelength-corrected to match the experimental short-wavelength UV λ_{max}. Note that ECD spectra for **4h**, **4i**, **4j** and **5i** were calculated for the enantiomers. Experimental and calculated spectra for **4h** and **4j** were taken from ref. 2b.

unambiguous assignment of the absolute configuration of the molecules studied. However, neither experimental nor theoretical ECD spectra for individual keto-*cis*-diols were similar between various compounds. This shows the effect of the polar substituents at C3 on the electronic properties of the enone chromophore. For example, the position of λ_{max} for 3-substituted enones in relation to hydrogen substituent changes in the sequence: Ph (+67) > I (+47) > OMe (+31) > Br (+18) ≥ Cl (+18) > Me (+14) > H (210 nm) > CF_3 (−12).

The electron withdrawing properties of the trifluoromethyl group are responsible for the unique 12 nm blue-shift of the UV maximum of keto *cis*-diol **4b**. The effect of the alkyl substituent (*i.e.* the methyl group) on the energies of the π–π* electronic transition is comparable to the effect of chlorine substituent. In the case of cyclohexenone *cis*-diols **4a**, **4d** and **4e** the substituent effect on the energy of the π–π* electronic transition correlates well with the halogen polarizability and is most significant for the iodine substituent. Substitution of the hydrogen atom at C3 in the 2-cyclohexenone skeleton by a methoxy group forms a classical push–pull system and this is reflected in the red-shift of the position and enhanced magnitude of the π–π* absorption maximum of ketodiol **4g**.

The conjugative effect of the phenyl substituent is clearly visible in the electronic spectrum of keto-*cis*-diol **4c**$_S$. This is also the most complex case, since the calculated ECD spectrum

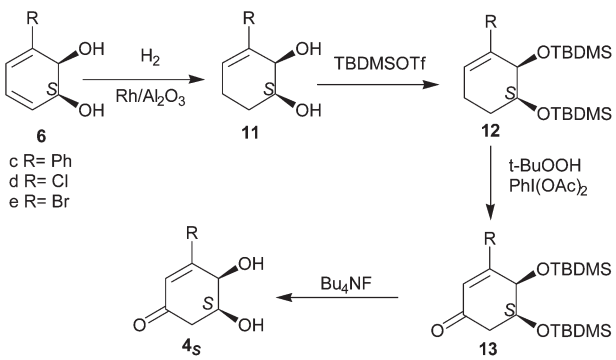

Scheme 5 Synthesis of cyclohexenone *cis*-diol metabolites **4c**$_S$–**4e**$_S$ obtained from the corresponding *cis*-dihydrodiols **6c**$_S$–**6e**$_S$.

does not satisfactorily fit the experimental one. The absolute configuration of compound **4c**$_S$ was however, independently established by the stereochemical correlation sequence shown in Scheme 5. As is usually the case, the discrepancy between the experiment and the computation of chiroptical properties resulted from either the incorrect computational reproduction of conformer population or from the method of ECD calculation, usually performed for "static" conformers. In the real molecule the Cotton effects originating from different rotamers of the phenyl

Table 1 Specific optical rotations for cyclohexenone *cis*-diols **4a–4j**, **5g** and **5i** measured in methanol solution and calculated at the PCM/B3LYP/Aug-cc-pVTZ level (values in parentheses)

Diol	589 nm		578 nm		546 nm		436 nm	
4a	−38[a]	(−224)	−37	(−238)	−42	(−290)	−61	(−922)
4b	−82	(−99)	−86	(−104)	−98	(−119)	−147	(−181)
4c	−20[b]	(−74)	−21	(−79)	−21	(−93)	+32	(−203)
4d	−52	(−110)	−54	(−116)	−63	(−133)	− 109	(−237)
4e	−45	(−60)	−47	(−62)	−55	(−70)	−96	(−104)
4f	−120	(−129)	−127	(−133)	−145	(−154)	−219	(−264)
4g	−103	(−128)	−109	(−136)	−129	(−163)	−286	(−370)
4h	+223	(−264)[cd]	+234	(−340)[cd]	+273	(−399)[cd]	+540	(−814)[cd]
4i	+59	(−105)[c]	+88	(−111)[c]	+110	(−135)[c]	+219	(−331)[c]
4j	+104[d]	(−108)[c]	+109	(−151)[cd]	+128	(−171)[cd]	+259	(−248)[cd]
5g	−92	(−92)	n.a.	(−95)	*n.a.*	(−102)	n.a.	(−81)
5i[c]	+92	(−151)[c]	n.a.	(−158)[c]	*n.a.*	(−181)[c]	n.a.	(−301)[c]

[a] Ref. 2*a*. [b] Ref. 2*c*. [c] Calculated for the enantiomer. [d] Ref. 2*b*.

ring are mutually cancelled, since the barrier to aromatic ring rotation around the C3–C_{Ar} bond is low. In the calculated ECD spectra the effect of the phenyl group is clearly visible because of the fixed conformation of the aromatic ring.

A further difficult case is represented by keto-*cis*-diol **4i**. The first and the third Cotton effects calculated for ***ent*-4i** are of opposite sign to these measured. The second Cotton effect is absent in the calculated spectrum due to mutual cancellation of π–π* electronic transition rotatory strengths of *M* and *P* conformers after Boltzmann averaging (see ESI‡). This example clearly shows that the populations of conformers *P*1 and *P*2 were underestimated. It is worth noting that the OR method for stereochemical assignment worked well in this case where measured OR values for compound **4i** and calculated OR values for compound ***ent*-4i** were found to be of opposite sign (Table 1).

The effect of conformation of the substituent at C3 is distinctively seen in the calculated optical rotations. An excellent example is the phenyl-substituted cyclohexenone *cis*-diol **4c** (see ESI, Table C2‡). Whereas OR values for the majority of conformers of the alkyl-substituted keto-*cis*-diols are negative (regardless *P* or *M* conformation),[2b] in the case of metabolite **4c** the rotation changes sign depending on the conformation of the phenyl group and assumes a negative sign for a positive value of angle ϕ and *vice versa*.

The results of measurement and calculation of optical rotation values for cyclohexenone-*cis*-diols are in agreement with configuration assignments obtained by ECD. Thus, the calculated and measured signs and magnitudes of specific optical rotations at four different wavelengths for **4a–4i** are in agreement with the assumed 5*S* configuration (Table 1, and also Table C2 in ESI‡).

This computational study shows that ECD spectra of cyclohexenone *cis*-diols **4a–4j**, **5g**, and **5i** reflect primarily the absolute configuration of these molecules at C4 and C5 and to a much lesser extent the preferred conformation of the molecules, in agreement with our previous results. Thus, a comparison of the results obtained from experimental and calculated ECD spectra of alkyl substituted cyclohexenone *cis*-diols **4** derived from the corresponding 3-substituted phenols (**1** R = Me, Et, *i*-Pr, *t*-Bu; R′ = H) [2b] with those of the current study (**1** R = Cl, Br, I, CF_3, Ph, OMe; R′ = H) confirmed that all are of identical (5*S*)-absolute configuration. Conversely, the three cyclohexenone *cis*-diols (**4** and **5**) formed from 2,5-disubstituted phenols (**1** R = Me, R′ = Cl; R = Me, R′ = Et; R = R′ = Me) were found to have opposite *cis*-diol absolute configurations at C4 and C5. However, cyclohexenone *cis*-diols **4g** and **5g** derived from the 2,5-disubstituted phenol **1g**, had the same configuration as those obtained from 3-substituted phenols **1**. This result could be explained in terms of similar relatively small size of the C6-F atom in *cis*-diols **4g** and **5g** and a C6-H atom in *cis*-diols **4a–4f**.

2.3 Chemoenzymatic synthesis of the cyclohexenone *cis*-diols $4c_S$, $4d_S$ and $4e_S$ from *cis*-dihydrodiols 6

The cyclohexenone *cis*-diols **4** have generally proved to be more stable than the corresponding benzene *cis*-dihydrodiols **6** and most can be stored at ambient temperatures for extended periods without significant decomposition. Although a range of cyclohexenone *cis*-diols **4** and **5** is now available from TDO-catalysed biotransformation of substituted phenols, the isolated yields of cyclohexenone *cis*-diols vary due to competing biosynthetic pathways.[2a–c] Thus the yield of *cis*-diol metabolite $\mathbf{4c_S}$ (28%)[2c] was reduced by formation of the alternative *cis*-dihydrodiol product **6** (R = 3–HO·C_6H_4, 10%).[2c] Similarly cyclohexenone *cis*-diols $\mathbf{4d_S}$ and $\mathbf{4e_S}$ found during the current study, proved to be minor metabolites (≤5% isolated yield) compared with the corresponding dominant catechol bioproducts. In order to generate sufficient quantities of metabolites $\mathbf{4c_S}$, $\mathbf{4d_S}$ and $\mathbf{4e_S}$ for stereochemical correlation studies, a chemoenzymatic route, based on the more readily available substituted benzene *cis*-dihydrodiols **6**, was developed (Scheme 5).

The *cis*-tetrahydrodiols **11c–11e** were obtained in good yield (>85%) by partial hydrogenation from the corresponding *cis*-dihydrodiols $\mathbf{6c_S}$–$\mathbf{6e_S}$ using Pd/C, Rh/Al_2O_3 or Rh/graphite catalysts and were available from earlier studies.[4,10a–c] While preferential protection of the pseudoaxial C1–OH group was found using *tert*-butyldimethylsilyl chloride, silylation of both OH groups in compounds **11c–11e** was achieved in excellent yields (>90%) by treatment with *tert*-butyldimethylsilyl triflate in the presence of triethylamine base to yield the diTBDMS derivatives **12c–12e**.

Using the method of Zhao and Yeung,[11] oxidation at the allylic (C5) position of the protected *cis*-tetrahydrodiols **12c–12e** gave the corresponding protected ketones **13c–13e**. This allylic oxidation step was achieved using a combination of diacetoxyiodobenzene and *tert*-butyl hydroperoxide [$PhI(OAc)_2$, *t*-BuO_2H], to generate *tert*-butylperoxy radical as *in situ* oxidant but the oxidation proved difficult to drive to completion. Although the protected cyclohexenone *cis*-diols **13c–13e** were only isolated in relatively low yields (37–42%), based on recovered starting material **12c–12e** after chromatography, the yields were estimated to be *ca.* 60%.

The final step involved deprotection of silyl ethers **13c–13e** to give cyclohexenone *cis*-diols $\mathbf{4c_S}$–$\mathbf{4e_S}$ which proved to be identical to the metabolites derived from the corresponding phenols **1c–1e**. Although the cyclohexenone *cis*-diols $\mathbf{4c_S}$–$\mathbf{4e_S}$ were much more stable than the corresponding dihydrodiols **6c–6e** at ambient temperature, under the deprotection conditions used for diTBDMS derivatives (tetrabutylammonium fluoride/THF), they proved to be less stable and this resulted in only modest isolated yields (29–52%). To improve the yield in the final step alternative *cis*-diol protecting groups are currently under investigation.

The stereochemical correlation of *cis*-dihydrodiols $\mathbf{6c_S}$–$\mathbf{6e_S}$ with the corresponding cyclohexenone *cis*-diols $\mathbf{4c_S}$–$\mathbf{4e_S}$, and X-ray crystallographic analyses of cyclohexenone *cis*-diols $\mathbf{4a_S}$,[2a] $\mathbf{4h_R}$,[2a] $\mathbf{4g_R}$ and $\mathbf{4i_R}$, provide unequivocal methods for the assignment of their stereochemistry. As the same absolute configurations were also assigned by the chiroptical methods, the validity of the ECD and OR approach for the determination of configuration of these, and other members of the cyclohexenone *cis*-diol family of metabolites *e.g.* $\mathbf{4f_S}$, has been further confirmed.

When combined with the earlier reports of the dioxygenase-catalysed formation of cyclohexenone *cis*-diol bacterial metabolites **4** from the corresponding monophenols,[2a–c] and a biphenol (3,3′-biphenol),[12a,b] addition of three further family members (R = H, CN, CO_2Me) obtained by chemoenzymatic synthesis,[2a] and the isolation of the fungal metabolites chlorosphaeropsidone and *epi*-chlorosphaeropsidone,[6] more than twenty five metabolites of this family have now been identified. From this study, it appears that this is a relatively common dioxygenase-catalysed metabolic pathway for 3-substituted and 2,5-disubstituted phenols. Although cyclohexenone *cis*-diol metabolites have also been isolated from the biotransformation of 2-substituted phenols (ref. 2*a* and unpublished data), to date none have yet been isolated from 4-substituted phenols.

2.4 Predictive models for TDO-catalysed *cis*-dihydroxylation of phenols

The phenol metabolites **4** and **5** discussed herein can be divided into two groups each with opposite absolute *cis*-diol configurations *i.e.* $\mathbf{4a_S}$–$\mathbf{4g_S}$, $\mathbf{5g_R}$ and $\mathbf{4h_R}$–$\mathbf{4j_R}$, $\mathbf{5i_R}$ (Scheme 1). In contrast the *cis*-dihydrodiol metabolites derived from monosubstituted (**6**) and *ortho* or *meta* disubstituted benzenes have consistently been found to possess the same absolute configuration. They were also found to be enantiopure (>98% ee) with the only exception being those derived from fluorobenzene or difluorobenzene substrates with slightly lower ee values.[3a–n]

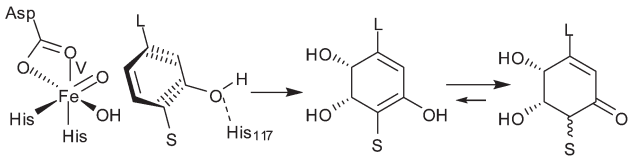

Scheme 6 TDO-catalysed oxidation of *meta*-phenols (S = H) or 2-fluoro-5-methyl phenol (S = F) to yield cyclohexenone *cis*-diols.

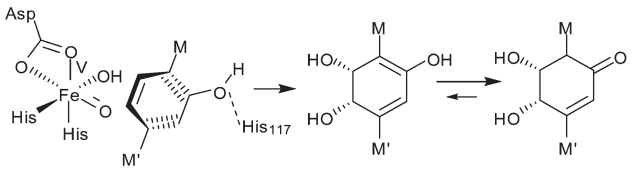

Scheme 7 TDO-catalysed oxidation of 2,5-disubstituted phenols to yield cyclohexenone *cis*-diols.

Simple predictive models have been developed for the TDO-catalysed *cis*-dihydroxylation of a large number of mono- and di-substituted benzenes, polycyclic arenes and azaarenes,[3f,k] and *meta*-phenols,[2c] to yield enantiopure *cis*-dihydrodiols of identical absolute configuration. It is, however, more difficult to rationalize the enantiomeric preference shown by the TDO enzyme when producing cyclohexenone *cis*-diol metabolites of opposite absolute configurations (*e.g.* $\mathbf{4a_S}$–$\mathbf{4g_S}$, $\mathbf{5g_R}$ and $\mathbf{4h_R}$–$\mathbf{4j_R}$, $\mathbf{5i_R}$). Our initial attempts to account for the enantiomeric preferences are shown in Schemes 6 and 7. These models are based on the assumption that dominant factors include: (i) the differential in the relative size of spherically symmetrical substituents or conformational preference of planar substituents *i.e.* large (L), medium (M) and small (S), (ii) flexibility in the relative position of the phenolic OH group which may interact with the proximate positively charged imidazole ring of histidine 311 in the active site of TDO[2c,13a–d] and (iii) the approach of the oxidant[13c,14] resulting in *cis*-dihydroxylation occurring on the lower face of the benzene ring. In the absence of any unequivocal evidence for the precise nature of the TDO oxidant, the (hydroxo)oxo iron (v) intermediate [HO–Fe^{V}═O] species appears to be one of the more favoured structures[13c,14] and has been used in Schemes 6 and 7.

The preferred absolute configurations of the cyclohexenone *cis*-diols shown in Scheme 6, are identical to those found for *cis*-dihydrodiol metabolites derived from both monocyclic and polycyclic arenes using TDO where a marked difference in large (L) and small (S) substituent size is also the dominant feature.[3f,k] Similarly, in 2,5-disubstituted phenol **1g**, where the smaller substituent was a fluorine atom, the cyclohexenone *cis*-diol product **4g** had the same absolute configuration as those derived from 3-substituted phenols. To date three examples of cyclohexenone *cis*-diols **4h–4j** (Scheme 7), having the opposite absolute configurations, have been isolated and in each case the differential between medium sized substituents *e.g.* Me, Et and Cl, was either small (M and M′ in **4i** and **4j**) or absent (M═M′, **4h**). In

this case other factors including substrate orientation in the TDO active site relative to histidine 311 and the (hydroxo)oxo iron (v) oxidant may also be important.

3. Conclusion

A series of 3-substituted (**1d–1f**) and 2,5-disubstituted phenols (**1g**, **1i** and **1j**) have been *cis*-dihydroxylated to yield the corresponding enantiopure cyclohexenone *cis*-diols *i.e.* **4d$_S$–4f$_S$**, **4g$_R$**, **4i$_R$**, **4j$_R$**, **5g$_R$** and **5i$_R$** with TDO as biocatalyst in *P. putida* UV4. All cyclohexenone *cis*-diols were found to be enantiopure with some being isolated as diastereoisomers *e.g.* **4** and **5** and some as enantiomers *e.g. cis*-diols **4$_S$** and **4$_R$** with opposite absolute configurations. The structures and absolute configurations of these chiral metabolites were determined using a combination of NMR and ECD spectroscopy, OR measurements, X-ray crystallography and stereochemical correlation methods. A chemoenzymatic synthesis route to cyclohexenone *cis*-diols **4**, from the more readily available non-hydroxylic monosubstituted benzene *cis*-dihydrodiols **6**, has been developed. An empirical model has been proposed, to allow prediction of the absolute configuration of cyclohexenone *cis*-diols **4** and **5** expected from the TDO-catalysed *cis*-dihydroxylation of the corresponding phenol substrates **1**.

4. Experimental

^{1}H and ^{13}C NMR spectra were recorded on Bruker Avance 400, DPX-300 and DRX-500 instruments. Chemical shifts (δ) are reported in ppm relative to $SiMe_4$ and coupling constants (J) are given in Hz. Mass spectra were run at 70 eV, on a VG Autospec Mass Spectrometer, using a heated inlet system. Accurate molecular weights were determined by the peak matching method, with perfluorokerosene as the standard. ECD spectra were recorded in spectroscopic grade acetonitrile using a JASCO J-720 instrument. A PerkinElmer 341 polarimeter was used for optical rotation ($[\alpha]_D$) measurements (*ca*. 20 °C). The methods used and results obtained from the calculations of ECD spectra and OR values are presented in the ESI.‡

Flash column chromatography and preparative layer chromatography (PLC) were performed on Merck Kieselgel type 60 (250–400 mesh) and $PF_{254/366}$ plates respectively. Merck Kieselgel type $60F_{254}$ analytical plates were employed for TLC. All phenol substrates and catechol bioproducts were available from commercial sources or from past studies.[4,5] The general procedure reported earlier for the biotransformation and isolation of metabolites of phenols **1a–1c**, **1h** and other phenol substrates, using whole cells of *P. putida* UV4,[2c] was utilized for small scale (0.2–1.0 g) biotransformation of phenols **1d–1g**, **1i** and **1j**. Catechol bioproducts were all known compounds and were identified by spectroscopic comparison with authentic samples.

(i) Biotransformation of 3-chlorophenol 1d

The crude mixture of metabolites separated by PLC contained mainly catechol **2d** and cyclohexenone *cis*-diol **4d$_S$** as the minor metabolite.

(4*S*,5*S*)-3-Chloro-4,5-dihydroxycyclohex-2-enone 4d$_S$. Pale yellow semi solid (0.038 g, 4%); R_f (0.29, 75% EtOAc in hexane); $[\alpha]_D$ − 52 (*c* 1.58, MeOH); HRMS (EI): Found M^+, 162.0071 requires $C_6H_7O_3{}^{35}Cl$ 162.0078; ^{1}H-NMR (400 MHz, CD_3OD) δ_H 2.61 (1 H, dd, *J* 16.5, 3.9, 6-H), 2.69 (1 H, dd, *J* 16.5, 7.2 Hz, 6′-H), 4.24 (1 H, ddd, *J* 7.2, 3.9, 3.6, 5-H), 4.44 (1 H, dd, *J* 3.6, 0.9, 4-H), 6.23 (1H, d, *J* 0.9, 2-H); ^{13}C-NMR (100 MHz, CD_3OD) δ_C 43.2, 69.6, 72.3, 129.4, 159.8, 197.2; LRMS (EI): 162 (M^+, 5%), 144 (18), 131 (53), 120 (32), 118 (100); IR (KBr) ν_{max}/cm^{-1} 3400 (OH), 1676 (C═O).

(ii) Biotransformation of 3-bromo-phenol 1e

The major metabolite isolated after PLC separation of the crude mixture of bioproducts was catechol **2e** and cyclohexenone *cis*-diol **4e$_S$** as a minor metabolite.

(4*S*,5*S*)-3-Bromo-4,5-dihydroxycyclohex-2-enone 4e$_S$. White crystals (0.054 g, 6%); m.p. 82–83 °C ($CHCl_3$–hexane); R_f 0.31 (75% EtOAc in hexane); $[\alpha]_D$ − 45 (*c* 1.08, MeOH); HRMS (EI): Found M^+, 205.9575 requires $C_6H_7O_3{}^{79}Br$ 205.9579; ^{1}H-NMR (400 MHz, CD_3OD) δ_H 2.62 (1 H, dd, *J* 16.4, 4.1, 6-H), 2.68 (1 H, dd, *J* 16.4, 7.1, 6′-H), 4.24 (1 H, ddd, *J* 7.1, 4.1, 3.5, 5-H), 4.50 (1 H, dd, *J* 3.5, 1.0, 4-H), 6.48 (1 H, d, *J* 1.0, 2-H); ^{13}C-NMR (100 MHz, CD_3OD) δ_C 43.2, 69.6, 73.5, 133.6, 152.9, 196.7; LRMS (EI): 208 (M^+, 3%), 206 (3), 190 (15), 188 (16), 164 (97), 162 (100), 136 (62), 134 (65); IR (KBr) ν_{max}/cm^{-1} 3399 (OH), 1654 (C═O).

(iii) Biotransformation of 3-methoxyphenol 1f

The major metabolite **4f$_S$** crystallised out from a mixture of several uncharacterised minor compounds using ethyl acetate.

(4*S*,5*S*)-4,5-Dihydroxy-3-methoxycyclohex-2-enone 4f$_S$. Colourless crystals (0.7 g, 55%); m.p. 128–129 °C dec. (EtOAc); R_f 0.11 (EtOAc); $[\alpha]_D$ − 120 (*c* 0.5, MeOH); HRMS (ES): Found $(M + H)^+$, 159.0650 requires $C_6H_{11}O_4$ 159.0657; ^{1}H-NMR (400 MHz, CD_3OD) δ_H 2.50 (1 H, dd, *J* 16.5, 4.1, 6-H), 2.66 (1 H, dd, *J* 16.5, 8.6, 6′-H), 3.78 (3 H, s, OMe), 4.12 (1 H, ddd, *J* 8.6, 4.1, 3.5, 5-H), 4.33 (1 H, d, *J* 3.5, 4-H), 5.39 (1 H, s, 2-H); ^{13}C- NMR (100 MHz, CD_3OD) δ_C 42.2, 57.1, 69.0, 70.3, 102.8, 178.5, 200.1; LRMS (ES): 159 ($[M + H]^+$, 77%), 181 (45), 317 (18), 339 (100), 497 (15); IR (film) ν_{max}/cm^{-1} 3362 (OH), 1605 (C═O).

(iv) Biotransformation of 2-fluoro-5-methylphenol 1g

Biotransformation of phenol **1g** gave, after PLC separation, two major cyclohexenone *cis*-diol metabolites **4g$_R$** and **5g$_R$** in the ratio 2.2 : 1.

(4*R*,5*R*,6*R*)-6-Fluoro-4,5-dihydroxy-3-methylcyclohex-2-enone 4g$_R$. Colourless crystalline solid (0.091 g, 14%); m.p. 139–140 °C ($CHCl_3$–MeOH); R_f (0.16, 40% EtOAc in hexane, 4 elutions); $[\alpha]_D$ − 103.0 (*c* 0.9, MeOH); HRMS (EI): Found M^+, 160.0536 requires $C_7H_9O_3F$ 160.0530; ^{1}H-NMR (400 MHz, $CDCl_3$) δ_H 2.09 (3 H, dd, *J* 2.5, 1.2, Me), 2.65 (1 H, d, *J* 2.7, OH), 2.83 (1 H, d, *J* 10.9, OH), 4.46 (1 H, d, *J* 10.9, 4-H), 4.70

(1 H, dddd, *J* 9.7, 3.0, 3.0, 3.0, 5-H), 4.97 (1 H, dd, *J* 46.9, 2.6, 6-H), 5.96–5.99 (1 H, m, 2-H); ^{13}C-NMR (100 MHz, $CDCl_3$) δ_C 20.2, 70.1 (d, *J* 8.6) 72.96 (d, *J* 17.4), 91.30 (d, *J* 192.4), 124.4 (d, *J* 1.4), 160.5 (d, *J* 1.5), 191.2 (d, *J* 15.8); ^{19}F-NMR (376 MHz, $CDCl_3$) δ_F 202.2 (1 F, dddd, *J* 46.9, 10.5, 6.1, 1.5); LRMS (EI): 160 (M^+, 3%), 142 (45), 125 (15), 98 (100); IR (KBr) ν_{max}/cm^{-1} 3255 (OH), 1682 (C═O).

Crystal data for 4g$_R$. $C_7H_9FO_3$, *M* = 160.1, orthorhombic, *a* = 4.641(2), *b* = 10.535(3), *c* = 15.936(4) Å, *U* = 779.2(3) Å^3, *T* = 298(2) K, space group $P2_12_12_1$ (no. 19), Mo-Kα radiation, λ = 0.71073Å, *Z* = 4, *F*(000) = 336, D_x = 1.365 g cm^{-3}, μ = 0.121 mm^{-1}, Bruker SMART CCD diffractometer, φ/ω scans, 4.6° < 2θ < 55.9°, measured/independent reflections: 3415/1482, R_{int} = 0.030, direct methods solution, full-matrix least squares refinement on F_o^2, anisotropic displacement parameters for non-hydrogen atoms; all hydrogen atoms located in a difference Fourier synthesis but included at positions calculated from the geometry of the molecule using the riding model, with isotropic vibration parameters. R_1 = 0.045 for 1205 data with $F_o > 4\sigma(F_o)$, 103 parameters, ωR_2 = 0.115 (all data), GoF = 1.05, $\Delta\rho_{min,max}$ = −0.15/0.15 e Å^{-3}. CCDC 852568. The absolute configuration is not determined in this analysis but is confirmed as (4*R*,5*R*,6*R*) by correlation with the structure analysis of the camphanate derivative **4g$_{R\text{-cam}}$**.

(1*S*,4*R*)-1-(1*R*,2*R*,6*R*)-6-Fluoro-2-hydroxy-3-methyl-5-(oxocyclohex-3-enyloxymethyl)-4,7,7-trimethyl-2-oxabicyclo[2.2.1]heptan-3-one 4g$_{R\text{-cam}}$. A stirred solution of ketodiol **4g$_R$** (0.040 g, 0.25 mmol), in dry pyridine (0.5 ml), was treated with (−)-(*S*)-camphanic chloride (0.070 g, 0.32 mmol) at room temperature. After stirring the reaction mixture for 3 h at room temperature, the pyridine was distilled off under reduced pressure, the residue extracted with EtOAc (25 ml), the extract successively washed with 5% aq. $NaHCO_3$ solution (20 ml), water (15 ml) and then dried (Na_2SO_4). The solvent was removed under reduced pressure and the residue purified by PLC (80% EtOAc in hexane) to yield camphanate **4g$_{R\text{-cam}}$** as a colourless crystalline solid (0.070 g, 82%); m.p. 125–126 °C (CH_2Cl_2–MeOH); R_f (0.55, 80% EtOAc in hexane); $[\alpha]_D$ − 46 (*c* 0.45, MeOH); HRMS (EI): Found M^+, 340.1340 requires $C_{17}H_{21}O_6F$ 340.1322; ^{1}H-NMR (400 MHz, CD_3OD) δ_H 0.92 (3 H, s, CMe_2), 1.00 (3 H, s, CMe_2), 1.06 (3 H, s, *Me*CCH_2), 1.56–1.64 (1 H, m, MeCCH_2), 1.90–2.03 (2 H, m, MeCCH_2 and CH_2CO), 2.06 (3 H, t, *J* 1.3, CHC*Me*), 2.29–2.37 (1 H, m, CH_2CO), 4.81–4.84 (1 H, br m, 2-H), 5.38 (1 H, dd, *J* 45.4, 2.8, 6-H), 5.96–6.00 (1 H, m, 4-H), 6.07 (1 H, dt, *J* 8.8, 3.1, 1-H); ^{13}C-NMR (100 MHz, CD_3OD) δ_C 9.8, 16.6, 16.9, 20.1, 30.0, 31.5, 55.6, 56.1, 69.4 (d, *J* 8.7 Hz), 77.6 (d, *J* 16.3), 90.4 (d, *J* 195.2 Hz), 92.9, 124.7 (d, *J* 1.3), 164.7, 168.1, 180.2, 193.3 (d, *J* 15.7 Hz); ^{19}F-NMR (376 MHz, CD_3OD) δ_F −204.7 (1 F, dddd, *J* 45.7, 8.9, 6.0, 2.2); LRMS (EI): 340 (M^+, 4%), 264 (27), 219 (95), 131 (65), 69 (100); IR (film) ν_{max}/cm^{-1} 3275 (OH), 1784 (C═O).

Crystal data for 4g$_{R\text{-cam}}$. $C_{17}H_{21}FO_6$, *M* = 340.3, monoclinic, *a* = 8.272(1), *b* = 10.422(2), *c* = 10.053(2) Å, β = 106.38(1)°, *U* = 831.4(2) Å^3, *T* = 293(2) K, space group $P2_1$ (no. 4), Mo-Kα radiation, λ = 0.71073Å, *Z* = 2, *F*(000) = 360, D_x = 1.359 g cm^{-3}, μ = 0.109 mm^{-1}, Bruker P4 diffractometer, ω scans, 4.2° < 2θ < 50.0°, measured/independent reflections: 2103/1723, R_{int} = 0.019, direct methods solution, full-matrix least squares refinement on F_o^2, anisotropic displacement parameters for non-hydrogen atoms; all hydrogen atoms located in a difference Fourier synthesis but included at positions calculated from the geometry of the molecule using the riding model, with isotropic vibration parameters. R_1 = 0.028 for 1619 data with $F_o > 4\sigma(F_o)$, 223 parameters, ωR_2 = 0.081 (all data), GoF = 1.03, $\Delta\rho_{min,max}$ = −0.13/0.17 e Å^{-3}. CCDC 852569. The absolute configuration is established as (4*R*,5*R*,6*R*) relative to the known absolute configuration of the (1′*S*)-camphanate group.

(4*R*,5*R*,6*S*)-6-Fluoro-4,5-dihydroxy-3-methylcyclohex-2-enone 5g$_R$. Colourless oil (0.028 g, 4%); R_f (0.21, 40% EtOAc in hexane, 4 elutions); $[\alpha]_D$ − 92 (*c* 1.2, MeOH); HRMS (EI): Found $(M - H_2O)^+$, 142.0423 requires $C_7H_9O_3F$ 142.0430; ^{1}H-NMR (400 MHz, $CDCl_3$) δ_H 2.15 (3 H, d, *J* 1.4, Me), 3.39 (1 H, br s, OH), 3.51 (1 H, br s, OH), 4.12 (1 H, ddd, *J* 10.5, 10.3, 4.2, 5-H), 4.41 (1 H, t, *J* 4.2, 4-H), 5.14 (1 H, dd, *J* 50.4, 10.3, 6-H), 5.99 (1 H, dq, *J* 3.8, 1.4, 2-H); ^{13}C-NMR (100 MHz, $CDCl_3$) δ_C 22.4, 70.8 (d, *J* 8.9), 71.0 (d, *J* 17.9), 91.4 (d, *J* 187.3), 126.8, 158.2, 192.3 (d, *J* 14.59); ^{19}F-NMR (376 MHz, $CDCl_3$) δ_F −214.1 (ddt, *J* 50.6, 10.4, 4.0); LRMS (EI): 142 ($[M - H_2O]^+$, 38%), 131 (35), 98 (100), 69 (52); IR (film) ν_{max}/cm^{-1} 3353 (OH), 1687 (C═O).

(v) Biotransformation of 5-chloro-2-methylphenol 1i

Phenol substrate **1i** gave a mixture of two bioproducts (13 : 1) which on separation by PLC yielded cyclohexenone *cis*-diols **4i$_R$** and **5i$_R$**.

(4*R*,5*R*,6*S*)-3-Chloro-4,5-dihydroxy-6-methylcyclohex-2-enone 4i$_R$. White crystals (0.058 g, 6%); m.p. 91–92 °C (EtOAc–hexane); R_f 0.17 (25% EtOAc in hexane, 5 elutions); HRMS (EI): Found M^+, 176.0225 requires $C_7H_9O_3{}^{35}Cl$ 176.0234; $[\alpha]_D$ + 59 (*c* 0.98, MeOH); ^{1}H-NMR (500 MHz, $CDCl_3$) δ_H 1.28 (3 H, d, *J* 6.9, Me), 2.59 (1 H, qd, *J* 6.9, 2.3, 6-H), 4.34 (1 H, dd, *J* 3.5, 2.3, 5-H), 4.55 (1 H, dd, *J* 3.5, 2.0, 4-H), 6.30 (1 H, d, *J* 2.0, 2-H); ^{13}C-NMR (100 MHz, $CDCl_3$) δ_C 11.0, 46.0, 71.2, 73.7, 128.3, 154.5, 195.8; LRMS (EI): 176 (M^+, 5%), 158 (5), 131 (21), 120 (30), 118 (100), 90 (52); IR (film) ν_{max}/cm^{-1} 3343 (OH), 1677 (C═O).

Crystal data for 4i$_R$. $C_7H_9ClO_3$, *M* = 176.6, monoclinic, *a* = 12.125(2), *b* = 4.870(2), *c* = 14.100(3) Å, β = 92.28(1)°, *U* = 832.0(3) Å^3, *T* = 293(2) K, space group $P2_1$ (no. 4), Mo-Kα radiation, λ = 0.71073Å, *Z* = 4, *F*(000) = 368, D_x = 1.410 g cm^{-3}, μ = 0.414 mm^{-1}, Bruker P4 diffractometer, ω scans, 4.3° < 2θ < 50.0°, measured/independent reflections: 2129/2024, R_{int} = 0.063, direct methods solution, full-matrix least squares refinement on F_o^2, anisotropic displacement parameters for non-hydrogen atoms; all hydrogen atoms located in a difference Fourier synthesis but included at positions calculated from the geometry of the molecules using the riding model, with isotropic vibration parameters. R_1 = 0.050 for 1400 data with $F_o > 4\sigma(F_o)$, 205 parameters, ωR_2 = 0.127 (all data), GoF = 1.04, $\Delta\rho_{min,max}$ = −0.20/0.21 e Å^{-3}. CCDC 852570. The absolute configuration is established as (4*R*,5*R*,6*S*) from the anomalous scattering arising from the chlorine atom; Flack parameter *x* = 0.08(13). The asymmetric

unit consists of two molecules, which do not differ significantly in conformation.

(4*R*,5*R*,6*R*)-3-Chloro-4,5-dihydroxy-6-methylcyclohex-2-enone 5i$_R$. Colourless oil (0.044 g, 0.5%); R_f 0.21 (25% EtOAc in hexane, 5 elutions); $[\alpha]_D$ + 92 (*c* 0.65, MeOH); HRMS (EI): Found M^+, 176.0226 requires $C_7H_9O_3{}^{35}Cl$ 176.0234; ^{1}H-NMR (500 MHz, $CDCl_3$) δ_H 1.24 (3 H, d, *J* 7.2, Me), 2.67 (1 H, br s, OH), 2.75 (1 H, dq, *J* 8.4, 7.2, 6-H), 3.11 (1 H, br s, OH), 3.94 (1 H, dd, *J* 8.4, 3.8, 5-H), 4.49 (1 H, d, *J* 3.8, 4-H), 6.28 (1 H, s, 2-H); ^{13}C-NMR (100 MHz, $CDCl_3$) δ_C 11.3, 44.8, 70.6, 72.8, 129.0, 154.0, 196.9; LRMS (EI): 176 (M^+, 3%), 142 (10), 131 (20), 120 (35), 118 (100), 92 (28), 90 (56); IR (film) ν_{max}/cm^{-1} 3318 (OH), 1677 (C=O).

(vi) Biotransformation of 2-ethyl-5-methyl-phenol 1j

PLC separation of the crude mixture of bioproducts gave cyclohexenone *cis*-diol **4j$_R$** as the major metabolite and catechol **2j** as the minor metabolite.

(4*S*,5*R*,6*S*)-6-Ethyl-4,5-dihydroxy-3-methylcyclohex-2-enone 4j$_R$. White crystalline solid (0.035 g, 12%); m.p. 78–79 °C (EtOAc–hexane); R_f 0.3 (75% EtOAc in hexane); $[\alpha]_D$ + 104 (*c* 1.1, MeOH); HRMS (LCMS): Found $(M + H)^+$, 171.1020 requires $C_9H_{15}O_3$ 171.1016; ^{1}H-NMR (400 MHz, $CDCl_3$) δ_H 0.98 (3 H, t, *J* 7.5, CH_2*Me*), 1.47 (1 H, ddq, *J* 14.4, 9.1, 7.5, C*H*$_2$Me), 2.02 (3 H, t, *J* 1.4, CHC*Me*), 2.04–2.14 (1 H, dqd, *J* 14.4, 7.5, 5.1, C*H*$_2$Me), 2.24 (1 H, ddd, *J* 9.1, 5.1, 3.2, 6-H), 4.34 (1 H, dd, *J* 3.5, 2.3, 4-H), 4.39–4.42 (1 H, m, 5-H), 5.88–5.90 (1 H, m, 2-H); ^{13}C-NMR (100 MHz, $CDCl_3$) δ_C 11.6, 18.0, 20.1, 53.1, 72.2, 72.3, 126.9, 158.4, 198.8; LRMS (LCMS): 193 ($[M + Na]^+$, 30%), 171 (100), 153 (20); IR (KBr) ν_{max}/cm^{-1} 3425 (OH), 1656 (C=O).

Synthesis of cyclohexenone *cis*-diols 4c–4e

Di-*tert*-butyldimethylsilyl ethers 12c–12e. NEt_3 (3 equivalents) was added to a solution of each *cis*-tetrahydrodiol (**11c–11e**, 1 equivalent) in dry CH_2Cl_2 (~5 ml), maintained at 0 °C, followed by the drop-wise addition of *tert*-butyldimethylsilyl triflate (2.2 equivalents). The reaction mixture was stirred at room temperature for 2 h, diluted with CH_2Cl_2 (15 ml) and then washed with ice cold water. The organic phase was separated, dried (Na_2SO_4), concentrated under reduced pressure and the residue obtained was purified by column chromatography (2% → 10% Et_2O in hexane) to yield di-TBDMS ethers (**12c–12e**).

(1*S*,2*R*-3-Phenylcyclohex-3-ene-1,2-diyl)*bis*(oxy)*bis*(*tert*-butyldimethylsilane) 12c. (1*S*,2*R*)-3-Phenylcyclohex-3-ene-1,2-diol **11c** (0.250 g, 1.31 mmol) yielded di-TBDMS ether **12c** as a colourless oil (0.510 g, 93%); R_f 0.4 (5% Et_2O in hexane); HRMS (EI): Found $(M - Me)^+$, 403.2499 requires $C_{23}H_{39}O_2Si_2$ 403.2483; $[\alpha]_D$ − 118 (*c* 1.11, $CHCl_3$); ^{1}H-NMR (400 MHz, $CDCl_3$) δ_H −0.32 (3 H, s, $SiMe_2$), −0.04 (3 H, s, $SiMe_2$), 0.14 (3 H, s, $SiMe_2$), 0.15 (3 H, s, $SiMe_2$), 0.71 (9 H, s, CMe_3), 0.97 (9 H, s, CMe_3), 1.53–1.61 (1 H, m, 6-H), 2.05–2.16 (1 H, m, 5-H), 2.19–2.30 (1 H, m, 6′-H), 2.36 (1 H, ddd, *J* 18.4, 5.1, 6.4, 5′-H), 3.83–3.88 (1 H, m, 1-H), 4.55–4.57 (1 H, m, 2-H), 5.86 (1 H, t, *J* 3.8, 4-H), 7.21–7.35 (5 H, m, Ar); ^{13}C-NMR (100 MHz, $CDCl_3$) δ_C −4.9, −4.3, −4.2, −4.1, 18.5, 18.7, 24.3, 26.0 (3C), 26.2, 26.4 (3C), 70.6, 73.5, 126.8 (2C), 126.9, 127.1, 128.3 (2C), 140.3, 141.5; LRMS (EI): 403 ($[M - Me]^+$, 2%), 361 (30), 260 (19), 203 (40), 155 (58), 147 (100).

(1*S*,2*S*-3-Chlorocyclohex-3-ene-1,2-diyl)*bis*(oxy)*bis*(*tert*-butyldimethylsilane) 12d. (1*S*,2*S*)-3-Chlorocyclohex-3-ene-1,2-diol **11d** (0.250 g, 1.68 mmol) gave di-TBDMS ether **12d** as a colourless oil (0.580 g, 91%); R_f 0.67 (5% Et_2O in hexane); $[\alpha]_D$ − 84 (*c* 1.02, $CHCl_3$); HRMS (ES): Found $(M + H)^+$, 377.2115 requires $C_{18}H_{38}O_2Si_2{}^{35}Cl$ 377.2099; ^{1}H-NMR (400 MHz, $CDCl_3$) δ_H 0.07 (3 H, s, $SiMe_2$), 0.08 (3 H, s, $SiMe_2$), 0.12 (3 H, s, $SiMe_2$), 0.15 (3 H, s, $SiMe_2$), 0.906 (9 H, s, CMe_3), 0.914 (9 H, s, CMe_3), 1.47–1.53 (1 H, m, 6-H), 1.91–2.12 (2 H, m, 5-H, 6′-H), 2.20 (1 H, dddd, *J* 18.1, 6.3, 5.0, 1.6, 5′-H), 3.75 (1 H, dt, *J* 6.2, 3.2, 1-H), 4.02 (1 H, d, *J* 3.2, 2-H), 5.79 (H, dd, *J* 4.8, 2.8, 4-H); ^{13}C-NMR (100 MHz, $CDCl_3$) δ_C −4.5, −4.2, −4.1, −4.05, 18.6, 18.9, 24.3, 25.3, 26.2 (3C), 26.3 (3C), 72.6, 74.2, 126.7, 132.4; LRMS (EI): 361 ($[M - Me]^+$, 2%), 319 (18), 217 (8), 189 (20), 161 (25), 147 (100) 113 (45).

(1*S*,2*S*-3-Bromocyclohex-3-ene-1,2-diyl)*bis*(oxy)*bis*(*tert*-butyldimethylsilane) 12e. (1*S*,2*S*)-3-Bromocyclohex-3-ene-1,2-diol **11e** (0.5 g, 2.59 mmol) furnished di-TBDMS ether **12e** as a colourless oil (0.980 g, 90%); R_f (0.68, 2% Et_2O in hexane); $[\alpha]_D$ − 68 (*c* 1.0, $CHCl_3$); HRMS (ES): Found $(M + H)^+$, 421.1598 requires $C_{18}H_{38}O_2Si_2{}^{79}Br$ 421.1594; ^{1}H-NMR (400 MHz, $CDCl_3$) δ_H 0.08 (3 H, s, $SiMe_2$), 0.09 (3 H, s, $SiMe_2$), 0.13 (3 H, s, $SiMe_2$), 0.19 (3 H, s, $SiMe_2$), 0.91 (9 H, s, CMe_3), 0.93 (9 H, s, CMe_3), 1.49–1.55 (1 H, m, 6-H), 1.93–2.03 (1 H, m, 5-H), 2.04–2.10 (1 H, m, 6′-H), 2.15–2.24 (1 H, m, 5′-H), 3.78 (1 H, dt, *J* 11.4, 3.2, 1-H), 4.12 (1 H, d, *J* 3.2, 2-H), 6.02 (1 H, dd, *J* 4.8, 2.5, 4-H); ^{13}C-NMR (100 MHz, $CDCl_3$) δ_C −4.5, −4.2, −4.0, −4.0, 18.6, 18.7, 24.0, 26.3 (3C), 26.35 (3C), 26.9, 72.7, 75.8, 122.7, 131.0; LRMS (EI): 365 ($[M - {}^tBu]^+$, 8%), 262 (5), 207 (15), 157 (18), 147 (100).

Di-*tert*-butyldimethylsilyl enones 13c–13e. *Tert*-butylhydroperoxide (6 M in decane, 5.5 equivalents) was added drop-wise to a stirred mixture of each di-TBDMS ether (**12c–12e**, 1 equivalent), butyl butyrate (~2 ml), diacetoxyiodobenzene (3 equivalents) and potassium carbonate (0.5 equivalents), maintained at 0 °C, and the solution was stirred over a period of 8 h. The reaction mixture was diluted with 5% Et_2O in hexane mixture (25 ml), the insoluble material filtered off and the filtrate concentrated. The residue left after distilling off the solvent was purified by column chromatography (2% → 5% Et_2O in hexane) followed by PLC to yield di-TBDMS enone (**13c–13e**).

(4*R*,5*S*)-4,5-*bis*(*tert*-Butyldimethylsilyloxy)-3-phenylcyclohex-2-enone 13c. Di-TBDMS **12c** (0.5 g, 1.19 mmol) gave enone **13c** as colourless crystalline solid (0.210 g, 41%); m.p. 74–75 °C (hexane); R_f 0.43 (10% Et_2O in hexane); $[\alpha]_D$ − 86 (*c* 0.9, $CHCl_3$); HRMS (ES): Found $(M + H)^+$, 433.2578 requires $C_{24}H_{40}O_3Si_2$ 433.2594; ^{1}H-NMR (400 MHz, $CDCl_3$) δ_H −0.24 (3 H, s, $SiMe_2$), 0.08 (3 H, s, $SiMe_2$), 0.13 (3 H, s, $SiMe_2$), 0.15 (3 H, s, $SiMe_2$), 0.72 (9 H, s CMe_3), 0.94 (9 H, s, CMe_3), 2.50 (1 H, dd, *J* 16.9, 4.6, 6-H), 2.99 (1 H, dd, *J* 16.9, 11.6, 6′-H), 4.18 (1 H, ddd, *J* 11.6, 4.6, 2.5, 5-H), 4.79 (1 H, d,

J 2.5, 4-H), 6.23 (1 H, s, 2-H), 7.41–7.51 (5 H, m, Ar); ^{13}C-NMR (100 MHz, $CDCl_3$) δ_C −5.0, −4.4, −4.3, −4.2, 18.4, 18.5, 25.8 (3C), 26.2 (3C), 41.0, 70.7, 70.8, 126.6, 127.1 (2C), 129.0 (2C), 130.2, 137.5, 158.8, 199.5; LRMS (EI): 417 ([M − Me]$^+$, 5%), 375 (51), 274 (20), 243 (19), 147 (100), 141 (30); IR (KBr) ν_{max}/cm^{-1} 1665 (C═O).

(4*S*,5*S*)-4,5-*bis*(*tert*-Butyldimethylsilyloxy)-3-chlorocyclohex-2-enone 13d. Di-TBDMS derivative **12d** (0.540 g, 1.4 mmol) gave enone **13d** as colourless crystalline solid (0.235 g, 42%); m.p. 59 °C (Et_2O–hexanes); R_f 0.49 (5% Et_2O in hexanes); $[\alpha]_D$ − 33 (*c* 1.03, $CHCl_3$); HRMS (EI): Found (M − CH_3)$^+$, 375.1579 requires $C_{17}H_{32}O_3Si_2$ ^{35}Cl 375.1573; ^{1}H-NMR (400 MHz, $CDCl_3$) δ_H 0.08 (3 H, s, $SiMe_2$), 0.09 (3 H, s, $SiMe_2$), 0.15 (3 H, s, $SiMe_2$), 0.17 (3 H, s, $SiMe_2$), 0.88 (9 H, s, CMe_3), 0.90 (9 H, s, CMe_3), 2.43 (1 H, dd, *J* 16.6, 3.9, 6-H), 2.84 (1 H, dd, *J* 16.6, 10.2, 6′-H), 4.12 (1 H, dt, *J* 10.2, 3.2, 5-H), 4.23–4.32 (1 H, m, 4-H), 6.17 (1 H, s, 2-H); ^{13}C-NMR (100 MHz, $CDCl_3$) δ_C −4.6, −4.5, −4.3, −4.25, 18.4, 18.5, 26.0 (3C), 26.0 (3C), 41.8, 70.3, 74.5, 128.9, 157.6, 195.7; LRMS (EI): 375 ([M − CH_3]$^+$, 3%), 333 (23), 232 (9), 147 (100); IR (KBr) ν_{max}/cm^{-1} 1676 (C═O).

(4*S*,5*S*)-3-Bromo-4,5-*bis*(*tert*-butyldimethylsilyloxy)cyclohex-2-enone 13e. Di-TBDMS derivative **12e** (0.750 g, 1.78 mmol) yielded enone **13e** as colourless crystalline solid (0.286 g, 37%); m.p. 58 °C (Et_2O–hexane); R_f 0.41 (7.5% Et_2O in hexane); $[\alpha]_D$ − 26 (*c* 0.86, $CHCl_3$); HRMS (ES): Found (M + H)$^+$, 435.1393 requires $C_{18}H_{36}O_3Si_2{}^{79}Br$ 435.1386; ^{1}H-NMR (400 MHz, $CDCl_3$) δ_H 0.09 (3 H, s, $SiMe_2$), 0.10 (3 H, s, $SiMe_2$), 0.17 (3 H, s, $SiMe_2$), 0.21 (3 H, s, $SiMe_2$), 0.89 (9 H, s, CMe_3), 0.92 (9 H, s, CMe_3) 2.45 (1 H, dd, *J* 16.5, 3.8, 6-H), 2.85 (1 H, dd, *J* 16.5, 10.3, 6′-H), 4.14 (1 H, br d, *J* 9.2, 5-H), 4.41 (1 H, d, *J* 1.9, 4-H), 6.43 (1 H, s, 2-H); ^{13}C-NMR (100 MHz, $CDCl_3$) δ_C −4.5, −4.3, −4.25, −4.1, 18.4, 18.6, 26.0 (3C), 26.1 (3C), 41.3, 70.4, 76.2, 128.5, 133.3, 195.4; LRMS (EI): 421 ([M − CH_3]$^+$, 3%), 379 (18), 278 (10), 213 (8), 147 (100); IR (KBr) ν_{max}/cm^{-1} 1674 (CbO)).

Cyclohexenone diols 4c$_S$–4e$_S$. A solution of each enone (**13c–13e**, 1 equivalent) in dry THF (~4 ml) was treated with tetrabutylammonium fluoride (1 M, THF, 3 equivalents) at 0 °C. After stirring the reaction mixture at room temperature for 3 h the solvent was removed under reduced pressure and the residue purified by PLC (75% EtOAc in hexanes) to yield cyclohexenone diol (**4c$_S$–4e$_S$**). In each case the spectral data and specific rotation ($[\alpha]_D$) value for the synthesised sample was identical to that of the corresponding metabolite (**4c$_S$–4e$_S$**).[2c]

(4*R*,5*S*)-4,5-Dihydroxy-3-phenylcyclohex-2-enone 4c$_S$. Enone **13c** (0.2 g, 0.46 mmol) furnished cyclohexenone diol **4c$_S$** as colourless crystalline solid (0.049 g, 52%).

(4*S*,5*S*)-3-Chloro-4,5-dihydroxycyclohex-2-enone 4d$_S$. Enone **13d** (0.2 g, 0.51 mmol) yielded cyclohexenone diol **4d$_S$** as colourless crystalline solid (0.024 g, 29%).

(4*S*,5*S*)-3-Bromo-4,5-dihydroxycyclohex-2-enone 4e$_S$. Enone **13e** (0.280 g, 0.64 mmol) gave cyclohexenone diol **4e$_S$** as colourless crystalline solid (0.040 g, 30%).

Acknowledgements

We gratefully acknowledge financial support from DEL (PBAM^{c}I), and thank Sheoliang Guan and Dany Leborgne for assistance with synthetic aspects of the programme. All calculations were performed at the Poznan Supercomputing and Networking Center.

Notes and references

1 (*a*) B. L. Goodwin, *Handbook of Biotransformations of Aromatic Compounds*, CRC Press LLC, Boca Raton, 2005, pp. 109–124; (*b*) R. C. Bayley, S. Dagley and D. T. Gibson, *Biochem. J.*, 1966, **101**, 293; (*c*) D. T. Gibson, V. Mahadevan and J. F. Davey, *J. Bacteriol.*, 1974, **119**, 930; (*d*) J. A. Buswell, *J. Bacteriol.*, 1975, **124**, 1399; (*e*) J. C. Spain and D. T. Gibson, *Appl. Environ. Microbiol.*, 1988, **54**, 1399; (*f*) F. K. Higson and D. D. Focht, *Appl. Environ. Microbiol.*, 1989, **55**, 946; (*g*) J. C. Spain, G. J. Zylstyra, C. K. Blake and D. T. Gibson, *Appl. Environ. Microbiol.*, 1989, **55**, 2648; (*h*) C. Hinterregger, R. Leitner, M. Loidl, A. Ferschl and F. Streichsbier, *Appl. Microbiol. Biotechnol.*, 1992, **37**, 252; (*i*) G. Bestetti, E. Galli, B. Leoni, F. Pelizzoni and G. Sello, *Appl. Microbiol. Biotechnol.*, 1992, **37**, 260; (*j*) K. Lee, *FEMS Microbiol. Lett.*, 2006, **255**, 316; (*k*) D. Kim, J. S. Lee, K. Y. Choi, Y.-S. Kim, J. N. Choi, S.-K. Kim, J.-C. Chae, G. Zlystra, C. H. Lee and E. Kim, *Enzyme Microb. Technol.*, 2007, **41**, 221.

2 (*a*) N. D. Sharma, C. C. R. Allen, J. F. Malone and D. R. Boyd, *Chem. Commun.*, 2009, 3633; (*b*) M. Kwit, J. Gawronski, D. R. Boyd, N. D. Sharma and M. Kaik, *Org. Biomol. Chem.*, 2010, **8**, 5635; (*c*) D. R. Boyd, N. D. Sharma, P. Stevenson, C. McRoberts, J. T. G. Hamilton, J. M. Argudo, H. Mundi, L. A. Kulakov and C. C. R. Allen, *Org. Biomol. Chem.*, 2011, **9**, 1479.

3 (*a*) D. A. Widdowson, D. W. Ribbons and S. D. Thomas, *Janssen Chim. Acta*, 1990, **8**, 3; (*b*) H. A. J. Carless, *Tetrahedron: Asymmetry*, 1992, **3**, 795; (*c*) G. N. Sheldrake, in *Chirality and Industry*, ed. A. N. Collins, G. N. Sheldrake and J. Crosby, John Wiley Ltd., Chichester, 1992, 127; (*d*) S. M. Brown and T. Hudlicky, in *Organic Synthesis: Theory and Applications*, ed. T. Hudlicky, JAI Press, Greenwich, 1993, vol. 2, p. 113; (*e*) S. M. Resnick, K. Lee and D. T. Gibson, *J. Ind. Microbiol.*, 1996, **17**, 438; (*f*) D. R. Boyd and G. N. Sheldrake, *Nat. Prod. Rep.*, 1998, **15**, 309; (*g*) T. Hudlicky, D. Gonzalez and D. T. Gibson, *Aldrichimica Acta.*, 1999, **32**, 35; (*h*) D. T. Gibson and R. E. Parales, *Curr. Opin. Biotechnol.*, 2000, **11**, 236; (*i*) D. R. Boyd, N. D. Sharma and C. C. R. Allen, *Curr. Opin. Biotechnol.*, 2001, **12**, 564; (*j*) R. A. Johnson, *Org. React.*, 2004, **63**, 117; (*k*) D. R. Boyd and T. D. H. Bugg, *Org. Biomol. Chem.*, 2006, **4**, 181; (*l*) K. A. B. Austin, M. Matveenko, T. A. Reekie and M. G. Banwell, *Chem. Aust.*, 2008, **75**, 3; (*m*) T. Hudlicky and J. W. Reed, *Synlett*, 2009, 685; (*n*) T. Hudlicky and J. W. Reed, *Chem. Soc. Rev.*, 2009, **38**, 3117.

4 V. Berberian, C. C. R. Allen, N. D. Sharma, D. R. Boyd and C. Hardacre, *Adv. Synth. Catal.*, 2007, **349**, 727.

5 D. R. Boyd, J. Blacker, B. Byrne, H. Dalton, M. V. Hand, S. Kelly, R. A. More O'Ferrall, S. N. Rao, N. D. Sharma, G. N. Sheldrake and H. Dalton, *J. Chem. Soc., Chem. Commun.*, 1994, 313.

6 (*a*) A. Evidente, L. Sparapano, A. Andolfi, G. Bruno, F. Giordano and A. Motta, *Phytopathol. Mediterr.*, 2000, **39**, 299; (*b*) A. Evidente, L. Sparapano, O. Fierro, G. Bruno, F. Giordano and A. Motta, *Phytochemistry*, 1998, **48**, 1139.

7 (*a*) J. Gawronski, M. Kwit, D. R. Boyd, N. D. Sharma, J. F. Malone and A. Drake, *J. Am. Chem. Soc.*, 2005, **127**, 4308; (*b*) D. R. Boyd, N. D. Sharma, G. P. Coen, P. Gray, J. F. Malone and J. Gawronski, *Chem.–Eur. J.*, 2007, **13**, 5804; (*c*) M. Kwit, N. D. Sharma, D. R. Boyd and J. Gawronski, *Chirality*, 2008, **20**, 609.

8 (*a*) R. D. Burnett and D. N. Kirk, *J. Chem. Soc., Perkin Trans. 1*, 1981, 1460; (*b*) J. K. Gawronski, *Tetrahedron*, 1982, **38**, 3; (*c*) N. Kirk, *Tetrahedron*, 1986, **42**, 777; (*d*) J. Gawronski, Conformations, Chiroptical and Related Spectral Properties of Enones, in *The Chemistry of Enones*, ed. S. Patai and Z. Rappoport, J. Wiley, 1989, ch. 3; (*e*) D. A. Lightner and J. E. Gurst, *Organic Conformational Analysis and Stereochemistry from Circular Dichroism Spectroscopy*, Wiley-VCH, 2000; (*f*) G. Snatzke, *Angew. Chem., Int. Ed. Engl.*, 1979, **18**, 363; (*g*) G. Snatzke, in *Fundamental Aspects and Recent Developments in Optical Rotatory Dispersion and Circular Dichroism*, ed. F. Ciardelli, P. Salvadori, Heyden, London, 1973, pp. 109–124; (*h*) G. Snatzke, *Tetrahedron*, 1965, **21**, 413;

(*d*) G. Snatzke, *Tetrahedron*, 1965, **21**, 421; (*j*) C. Djerassi, R. Records, E. Bunnenberg, K. Mislow and A. Moscowitz, *J. Am. Chem. Soc.*, 1962, **84**, 870; (*k*) W. B. Whalley, *Chem. Ind.*, 1962, 1024; (*l*) W. Hug and G. Wagniere, *Helv. Chim. Acta*, 1971, **54**, 633; (*m*) T. Liljefors and N. L. Allinger, *J. Am. Chem. Soc.*, 1976, **98**, 2745; (*n*) J. K. Gawronski, T. Liljefors and B. Nordén, *J. Am. Chem. Soc.*, 1979, **101**, 5515; (*o*) G. Snatzke, *Tetrahedron*, 1965, **21**, 439; (*p*) G. Snatzke, in *Optical Rotatory Dispersion and Circular Dichroism in Organic Chemistry*, ed. G. Snatzke, Sadtler Research Labs, Inc., Philadelphia, 1967, pp. 208–223; (*q*) H.-G. Kuball, S. Neubrech and A. Schönhofer, *Chem. Phys.*, 1992, **163**, 115; (*r*) H.-G. Kuball, B. Schultheis, M. Klasen, J. Frelek and A. Schönhofer, *Tetrahedron: Asymmetry*, 1993, **4**, 517; (*s*) J. Frelek, W. J. Szczepek, H. P. Weiss, G. J. Reiss, W. Frank, J. Brechtel, B. Schultheis and H.-G. Kuball, *J. Am. Chem. Soc.*, 1998, **120**, 7010; (*t*) J. Frelek, W. J. Szczepek, S. Neubrech, B. Schultheis, J. Brechtel and H.-G. Kuball, *Chem.–Eur. J.*, 2002, **8**, 1899; (*u*) A. W. Burgstahler and R. C. Barkhurst, *J. Am. Chem. Soc.*, 1970, **92**, 7601; (*v*) M. Kwit, P. Skowronek, J. Gawronski, J. Frelek, M. Woznica and A. Butkiewicz, *Some Inherently Chiral Chromophores – Empirical Rules and Quantum Chemical Calculations in Comprehensive Chiroptical Spectroscopy*, ed. N. Berova, R. Woody, K. Nakanishi and P. Polavarapu, Wiley, 2012, vol. 2, pp. 39–72.

9 (*a*) N. Harada and P. Stephens, *Chirality*, 2010, **22**, 229; (*b*) N. M. O'Boyle, A. L. Tenderholt and K. M. Langner, *J. Comput. Chem.*, 2008, **29**, 839.

10 (*a*) D. R. Boyd, N. D. Sharma, G. P. Coen, V. Ljubez, P. K. M. McGeehin and C. C. R. Allen, *Org. Biomol. Chem.*, 2007, **5**, 514; (*b*) D. R. Boyd, N. D. Sharma, M. V. Berberian, K. Dunne, C. Hardacre, M. Kaik, B. Kelly, J. F. Malone, S. T. McGregor and P. J. Stevenson, *Adv. Synth. Catal.*, 2010, **352**, 855; (*c*) M. Bell, D. R. Boyd, K. S. Dunne, J. F. Malone, B. Kelly and P. J. Stevenson, *Org. Biomol. Chem.*, 2012, **10**, 1388, DOI: 10.1039/c1ob06599h.

11 Y. Zhao and Y.-Y. Yeung, *Org. Lett.*, 2010, **12**, 2128.

12 (*a*) M. Sondossi, B. A. Lloyd, D. Barriault, M. Sylvestre and M. Simard, *Acta Crystallogr., Sect. C: Cryst. Struct. Commun.*, 1995, **51**, 491; (*b*) M. Sondossi, D. Barriault and M. Sylvestre, *Appl. Environ. Microbiol.*, 2004, **70**, 174.

13 (*a*) A. Karlsson, J. V. Parales, R. E. Parales, D. T. Gibson and H. Ramaswamy, *Science*, 2003, **299**, 1309; (*b*) T. D. Bugg, *Tetrahedron*, 2003, **59**, 7075; (*c*) T. D. Bugg and S. Ramaswamy, *Curr. Opin. Chem. Biol.*, 2008, **12**, 134; (*d*) R. Friemann, K. Lee, E. N. Brown, D. T. Gibson, H. Eklund and S. Ramaswamy, *Acta Crystallogr., Sect. D: Biol. Crystallogr.*, 2009, **65**, 24.

14 A. R. McDonald and L. Que, *Nat. Chem.*, 2011, **3**, 762.